Materials Performance and Characterization

Bryan Zuanetti,[1] Nathan Mutter,[2] and Ali P. Gordon[3]

DOI: 10.1520/MPC20130088

Multi-rate and Multi-modal Characterization of an Advanced Poly(etherimide): Ultem 1000

VOL. 3 / NO. 1 / 2014

Materials Performance and Characterization

doi:10.1520/MPC20130088 / Vol. 3 / No. 1 / 2014 / available online at www.astm.org

Bryan Zuanetti,[1] Nathan Mutter,[2] and Ali P. Gordon[3]

Multi-rate and Multi-modal Characterization of an Advanced Poly(etherimide): Ultem 1000

Reference

Zuanetti, Bryan, Mutter, Nathan, and Gordon, Ali P., "Multi-rate and Multi-modal Characterization of an Advanced Poly(etherimide): Ultem 1000," *Materials Performance and Characterization*, Vol. 3, No. 1, 2014, pp. 178–203, doi:10.1520/MPC20130088. ISSN 2165-3992

ABSTRACT

The key to the effective implementation of polymers in structural applications is an understanding of the mechanical response under a variety of conditions. In this study, an unreinforced poly(etherimide) (PEI) known as Ultem 1000 was characterized under quasi-static and high-strain-rate loading. Standard tension, compression, and torsion experiments were conducted in order to investigate the multi-regime response of this material. The elastic response of the material to multiple loading conditions was correlated using the Ramberg–Osgood model. The effects of thermal and mechanical rejuvenation processes on the mechanical response were investigated; the upper yield strength of the material was reduced, and the strain softening regime responsible for strain localization was largely eliminated. The fracture toughness of the material was evaluated using a Charpy impact test, and the mechanisms of failure were shown to be brittle. The high-strain-rate response of the material to uniaxial compression was evaluated by means of a miniaturized split Hopkinson pressure bar, and the strain-rate dependence of the material was modeled using the Ree–Eyring equations. Finally, a combination of the Ramberg–Osgood model and a novel model was employed to correlate the elastoplastic response of rejuvenated PEI to quasi-static mechanical loading.

Manuscript received November 11, 2013; accepted for publication February 10, 2014; published online June 23, 2014.

[1] Dept. of Mechanical & Aerospace Engineering, Univ. of Central Florida, Orlando, FL 32816-2450, United States of America, e-mail: Bzuanetti@knights.ucf.edu

[2] Dept. of Mechanical & Aerospace Engineering, Univ. of Central Florida, Orlando, FL 32816-2450, United States of America, e-mail: nathan.mutter@gmail.com

[3] Dept. of Mechanical & Aerospace Engineering, Univ. of Central Florida, Orlando, FL 32816-2450, United States of America, e-mail: apg@ucf.edu

Keywords
bilinear model, thermoplastics, experimental mechanics, dynamic response, toughness, ductility, Kolsky bar, glassy polymer, strain-rate sensitivity

Introduction

The development and production of robust polymers has increased the demand for thermoplastics in aerospace, automotive, medical, and defense applications. These polymers are sought after because of their excellent mechanical properties such as fracture toughness, specific strength, durability, and thermal and chemical resistance; however, applications for many of these materials are limited because of the lack of experimental mechanics data. In order to incorporate these materials in demanding designs, it is necessary to investigate the response of these polymers to a range of loading rates and conditions. A number of researchers have developed mechanical properties for poly(etherimide) (PEI), as well as other polymeric solids. In many cases, however, the focus was a single mode of mechanical response. Slight variations in the mechanical processing route strongly affect the mechanical responses of these materials. In the current study, a full characterization of PEI was conducted with emphasis on high strain rates.

Several researchers have investigated the dynamic response of polymeric solids. For example, Chou and colleagues employed a custom medium-strain-rate machine and a Kolsky bar apparatus to study poly(methyl methacrylate), cellulose acetate butyrate, polypropylene, and nylon 6 at a wide range of strain rates. It was noted that a positive dependence existed between the strength of the polymers and the rate of deformation [1]. Similar investigations were performed on a range of polymers by Walley and colleagues [2–4]. They too noted a positive strain-rate dependence in the yield strength of the polymers and went further to classify this relationship as one of three types. The first is a positively sloped linear relationship, the second is a positively sloped bilinear relationship, and the final relationship demonstrates a decrease in the strength of the material at a strain rate of approximately 10^3/s. The Eyring activation theory has been used by researchers to model the linear rate dependence of the yield strength in amorphous polymers [5,6]; however, for the bilinear case a modified version of this model known as the Ree–Eyring equation was developed, and this has been utilized by several researchers [7,8]. These techniques were utilized in this investigation to study the response of PEI to multi-rate deformation.

Unreinforced PEI resin, commonly referred to as Ultem 1000, is an amorphous thermoplastic with superb thermal, electrical, and mechanical properties. Because of its high specific strength and heat resistance, PEI has been used in a broad range of applications and in varying industrial fields. This material has been used in injection molding of a variety of interior and structural components in the Fokker 50 and 100 series aircraft [9]. It has been used for thermostat housing, transmission components, and headlight reflectors in automobiles [10]. In addition, PEI has been used to manufacture sterilization trays and surgical probes for the medical industry [11].

Researchers have studied the response of this thermoplastic in tribological, structural, and impact applications. Bijwe showed that the friction coefficient of PEI can be decreased with the addition of polytetrafluoroethylene (PTFE), and the wear

resistance can be increased by glass-fiber reinforcement [12]. Facca showed that it is possible to predict the linear elastic behavior of the material from thermodynamic processes [13]. Smmazcelik et al. studied the impact properties of carbon-fiber-reinforced PEI via the Izod impact experiment [14]. Novel production processes were developed by researchers in order to enhance the properties of PEI, such as the addition of alumina or silica nanoparticles to increase the ultimate strength or the fabrication of PEI nanofoams with a higher specific modulus and greater thermal resistivity than similar foams [15–17]. Natural aging and its effects on the static and fatigue characteristics of PEI have been investigated and were shown to critically decrease the strength and toughness of the material by promoting strain localization [18,19]. Also, models such as the elastoviscoplasticity theory by Ames and Anand and the Mulliken–Boyce model have been utilized to correlate the responses of similar amorphous polymers to multi-rate deformation [20–22]. Though the quasi-static properties of PEI have been investigated, only limited data are available in the literature, and no data are available relating to the high-strain-rate response and rate dependence of this material. The main focus of the current investigation was to evaluate the response of PEI to high strain rate deformation and the rate dependence of the material.

In the current study, the quasi-static response of PEI was evaluated through tension, compression, and torsion experiments. The effects of aging and rejuvenation on the mechanical properties of PEI were evaluated in compression and are discussed. The fracture toughness of the material in response to notched impact was evaluated using a Charpy impact test machine. The high-strain-rate response of the material to uniaxial compression was investigated using a miniaturized split Hopkinson pressure bar (MSHPB), and the strain-rate dependence of PEI is modeled using the Ree–Eyring equations. Finally, a novel model is proposed to correlate the mechanical response of rejuvenated PEI to quasi-static load. With regard to each test type, relevant literature is reviewed throughout this work.

Ultem 1000

PEI is a thermoplastic composed of repeating units of the large monomer $C_{37}H_{24}O_6N_{27}$. This material can be derived from the synthesis of tetracarboxylic dianhydride via polycondensation and purification of the molecule into the PEI monomer. The chemical composition and structure of PEI are illustrated in **Fig. 1** [23]. The

FIG. 1 (a) Molecular arrangement and (b) amorphous polymer chain of ULTEM 1000.

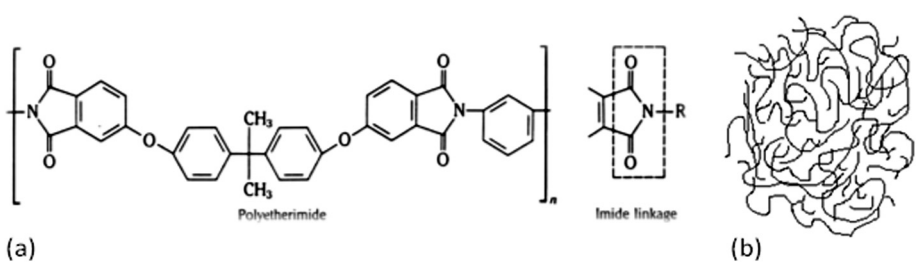

molecular structure of PEI is amorphous (i.e., the polymer chains lack long-range order).

Because PEI is composed of a large monomer, the resin exhibits excellent mechanical properties. The mechanical properties of Ultem 1000 with regard to quasi-static loading, fatigue, creep, and wear have been previously characterized; these are listed in **Table 1**. Like most amorphous polymers, Ultem 1000 exhibits an increase in strength in response to higher deformation rates [24,25]. Ultem can be filled with up to 45 vol. % glass fiber or PTFE, which increases strength at the expense of decreased flow properties.

Tensile Response

To study the tensile properties of the material, several uniaxial tensile experiments were performed on samples of ULTEM 1000. These experiments were performed using a universal test machine (MTS model Insight 5) with a 5-kN load cell operated at a crosshead velocity of 0.20 in./min (0.51 mm/min), as specified by ASTM D638 [26]. An axial extensometer (MTS model 634.11) was used to measure strain with a precision (specified by ASTM E83a [27]) of 0.001 % error. The test coupon and device are shown in **Figs. 2(*a*)** and **2(*b*)**, respectively. To properly define properties of the material such as Young's modulus, yield strength, ultimate strength, ductility, modulus, toughness, etc., the load-versus-displacement data from each test specimen were recorded and then averaged to eliminate any discrepancies.

Rectangular cross-sectional samples were milled from plate material into standard Type I specimens as specified by ASTM D638 [**Fig. 2(*b*)**]. The sample featured

TABLE 1

Quasi-static mechanical and thermal properties of Ultem 1000 [53].

Mechanical Properties	Value (English)	Value (SI)
Tensile modulus E_t	475 ksi	3.28 GPa
Compressive modulus E_c	480 ksi	3.31 GPa
Flexural modulus E_f	500 ksi	3.45 GPa
Poisson's ratio ν	0.36	0.36
Elongation (yield) ε_y, %	7.0	7.0
Tensile strength σ_{ut}	16.5 ksi	113.8 MPa
Compressive strength σ_{uc}	22 ksi	151.7 MPa
Shear strength σ_{su}	15 ksi	103.4 MPa
Flexural strength σ_{uf}	20 ksi	137.9 MPa
Elongation (fracture) ε_f, %	60	60
Izod impact resistance, notched	1.0 ft-lb/in.	0.034 J/m
Rockwell hardness, HRM	109	109
Physical Properties	Value (English)	Value (SI)
Specific gravity	1.28	1.28
Thermal Properties	Value (English)	Value (SI)
CTE-flow α_f	31 μin./in.-°F	55.8 μm/m-°C
Glass temperature T_g	419°F	215°C

FIG. 2 (a) Standard tensile sample dimensions. (b) Universal test frame with an axial extensometer attachment.

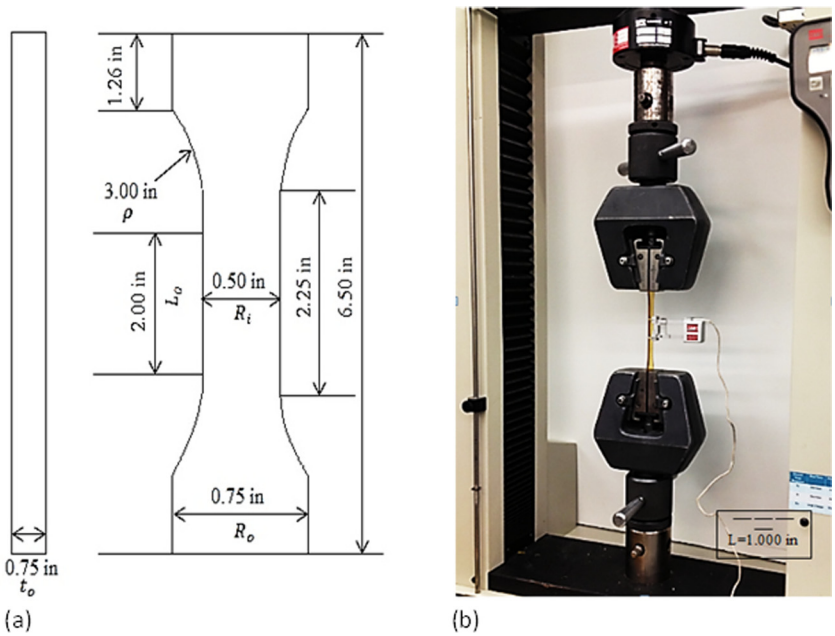

an outer radius R_o of 0.75 in. (19.1 mm), an inner radius R_i of 0.50 in. (12.7 mm), a gage section L_o of 2.0 in. (50.8 mm), and a thickness t of 0.094 in. (2.39 mm). To ensure that sample failure occurred within the gage section, a fillet with a radius ρ of 3.0 in. (76.2 mm) was introduced just outside the gage area.

MECHANICAL RESPONSE

Researchers have noted that the mechanical responses of several amorphous polymers are marked by four distinctive mechanical regimes before rupture: (i) linear elastic, (ii) nonlinear elastic, (iii) strain softening, and (iv) strain hardening [28–30]. The response of PEI is similar. Shown in **Fig. 3** are the tensile curves for PEI as it undergoes monotonic tensile deformation. The linear elastic regime is a result of van der Waals forces present during interactions between polymer chains as they slide with respect to one another [29]. The linear elastic regime is used to calculate the Young's modulus of the material, averaged at 470 ksi (3.24 GPa). As deformation continues, localization within the sample increases the level of stress until it finally overcomes the van der Waals forces and causes the linear response to become notably nonlinear; this occurs after the proportional limit (PL), found to be at 1 % engineering strain, is reached. At roughly 7.3 % engineering strain, the material exhibits a local maximum in stress considered the yield strength, and this value was averaged at 15.6 ksi (108 MPa). Upon plastic deformation the tensile curve exhibited a strain softening regime related to volume relaxation attributed to the physical aging process [31–33]. This mechanical response is a result of the reduction in mobility and increase in free volume caused by the polymer's slow shift toward equilibrium. The consequence of this process is strain localization that leads to a reduced stress-level requirement for continued deformation. The material then begins to strain-harden

FIG. 3 Mechanical response of the Ultem 1000 sample to uniaxial tensile load: (a) samples prior to plastic deformation; (b) fully deformed samples.

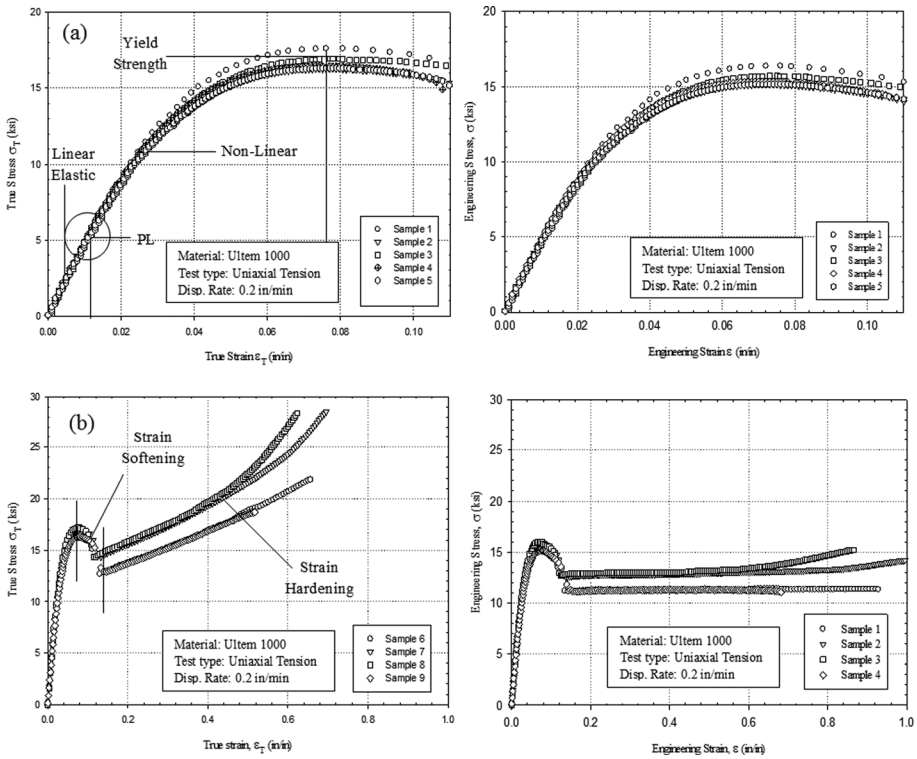

because of the alignment of the polymer chains in the direction of the force and the reduction of cavity density, which leads to an increased level of stress-level requirement for continued deformation [34]. Finally, the sample ruptures after reaching approximately 80 % engineering strain, at a stress of 13.6 ksi (89.6 MPa).

SAMPLE ANALYSIS

An analysis of the fractured tensile samples was performed in order to characterize the mechanisms of rupture. The fracture surfaces of several tensile samples are shown in **Fig. 4**. During deformation a stress concentration was the origination point for a slow-growing crack characterized by a mirror zone in the vicinity of the defect. Once the crack reached critical proportions, a mist zone characterized the transition between a slow-growing crack and a fast fracture. The stress levels generated by the test exceeded the load-bearing capacity of the sample, causing a fast fracture, and the presence of shear lips and dimples indicated a ductile overload. The fracture surface features mentioned above were consistent among the tensile samples. The fractographic analysis indicated that samples did fail at the load-bearing capacity of the material and displayed an adequate level of ductility under quasi-static conditions. A summary of the tensile properties of as-received Ultem 1000 is presented in **Table 2**, and these properties are averaged in **Table 3**. Samples attached with an axial extensometer were isolated from the average of ductility and toughness as a result of premature failure.

FIG. 4 Macro-scale fracture surfaces of the Ultem 1000 samples after uniaxial tension at a strain rate of 10^{-3}/s.

TABLE 2

Tensile properties of as-received Ultem 1000 at room temperature.

Sample Number	Ultimate Tensile Strength σ_{uts}, ksi (MPa)	Tensile Modulus E_t, ksi (MPa)	Upper Yield Strength σ_{uy}, ksi (MPa)	Lower Yield Strength σ_{ty}, ksi (MPa)	Strain at Upper Yield ε_y, %	Strain at Break ε_f, %	Elongation EL_y, %	Toughness u_t, ksi (MPa)	Attachment
1	16.4 (113)	475 (3275)	16.4 (113)	12.1 (83.4)	7.3	20	13	1.8 (12.4)	Extensometer
2	15.1 (104)	454 (3130)	15.1 (104)	11.6 (80.0)	7.1	24	17	2.1 (14.5)	Extensometer
3	15.7 (108)	456 (3144)	15.7 (108)	12.4 (85.5)	7.4	24	17	2.2 (15.2)	Extensometer
4	15.3 (105)	473 (3261)	15.3 (105)	12.0 (82.7)	7.2	20	13	1.9 (13.1)	Extensometer
5	15.2 (105)	463 (3192)	15.2 (105)	11.5 (79.3)	7.4	24	17	2.2 (15.2)	Extensometer
6	16.0 (110)	464 (3199)	16.0 (110)	12.9 (88.9)	7.2	87	80	11.6 (80.0)	None
7	15.8 (108)	469 (3233)	15.8 (108)	13.0 (89.6)	7.5	101	94	13.1 (90.3)	None
8	15.1 (104)	468 (3226)	15.1 (104)	11.2 (77.2)	7.1	93	86	10.6 (73.1)	None
9	15.2 (105)	441 (3040)	15.2 (105)	11.3 (77.9)	7.5	68	61	7.95 (54.8)	None

TABLE 3

Average tensile properties of Ultem 1000 at room temperature.

Mechanical Properties	Value (English Units)	Value (SI Units)
Tensile strength σ_{ut}	15.5 ksi	107 MPa
Tensile modulus E_t	465 ksi	3.2 GPa
Strain at yield ε_y, %	7.3	7.3
Strain at break ε_f, %	87.3	87.3
Elongation EL, %	80.3	80.3
Toughness U_t	10.8 ksi	74.5 MPa
Upper yield σ_{uy}	15.5 ksi	107 MPa
Lower yield σ_{ty}	12.0 ksi	82.7 MPa
0.02 % yield strength σ_{I2}	9.9 ksi	68.3 MPa
Ramberg–Osgood α	0.037	0.037
Ramberg–Osgood n	7.28	7.28

The Ultem 1000 samples exhibited an upper yield strength σ_{uy} of 15.5 ksi (107 MPa) and a lower yield strength σ_{ty} of 12.0 ksi (82.7 MPa) while elongating an average of 80.3 %. This material displayed significantly greater upper yield strength than other materials used for similar applications. Poly(carbonate) and poly(ether-ether-ketone) have strengths of around 8.7 ksi (60 MPa) and 14.5 ksi (100 MPa), respectively. Ultem 1000 maintains a high percentage of ductility once its upper yield strength has been exceeded; for this reason, the material is shown to maintain fracture toughness even at high stresses as compared to poly(carbonate) and poly(ether-ether-ketone).

Compressive Response

Quasi-static compression experiments were designed and performed in accordance with ASTM D695 [35]. Cylindrical samples were machined from as-received rod material to dimensions of 0.25 in. (6.35 mm) by 0.5 in. (12.7 mm), and they were subjected to compressive load at a crosshead velocity of 0.050 in./min (1.3 mm/min). These experiments were performed using an MTS Insight 5 mechanical testing unit, and the experimental setup is shown in **Fig. 5**. To prevent barreling of the samples, a

FIG. 5 (a) Standard compression test specimen dimensions. (b) Universal test frame with extensometer attachment.

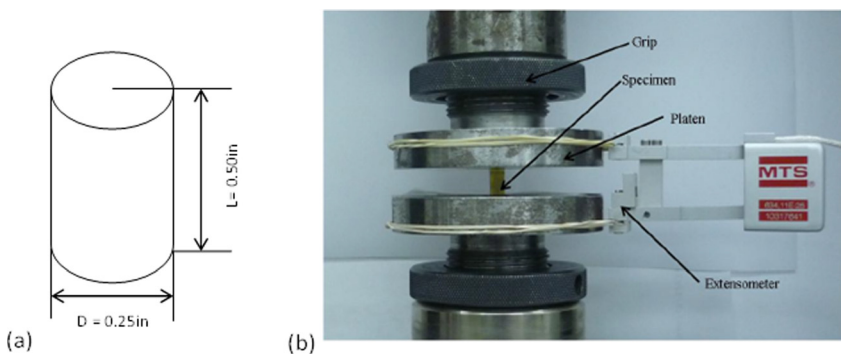

molybdenum disulfide film lubricant (Drislide Multi-Purpose) was applied on the platens of the mechanical testing unit.

RESULTS FROM EXPERIMENT

Similar to the quasi-static tensile behavior of as-received Ultem 1000, the compressive mechanical response is marked by four mechanical regimes: (i) linear elastic, (ii) nonlinear elastic, (iii) strain softening, and (iv) strain hardening. The compressive strength curve attained from this experiment, and properties of the curve are presented in **Fig. 6** and **Table 4**, respectively. The linear elastic regime is caused by the resistance to deformation due to the van der Waals forces that attract the polymer chains to one another. This regime lasts until about 1 % engineering strain and is used to calculate the compressive Young's modulus $E_{c'}$, which averages 480 ksi (3.31 GPa). Subsequent to the linear elastic behavior is the nonlinear elastic regime, caused by the polymer chains sliding with respect to one another [29,30]. At roughly 8.7 % engineering strain the material yields at 22 ksi (152 MPa). Upon yielding, the

FIG. 6

The mechanical response of Ultem 1000 to uniaxial compressive loading: (a) engineering and true responses; (b) mechanical regimes.

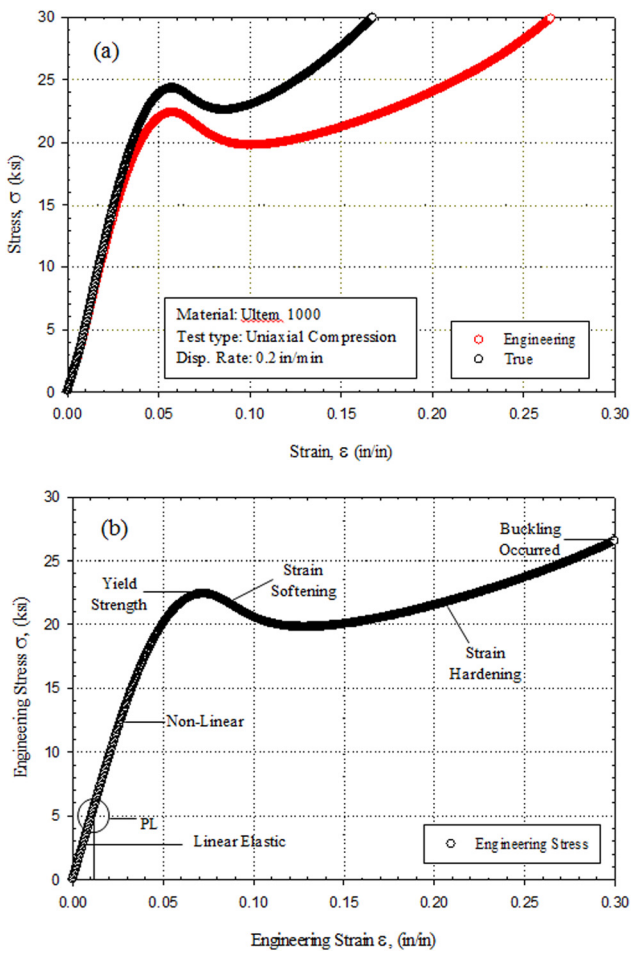

TABLE 4

Compressive properties of Ultem 1000 at room temperature.

Mechanical Properties	Value (English Units)	Value (SI Units)
Compressive modulus E_c	480 ksi	3.3 GPa
Strain at yield ε_{yc}, %	7.2	7.2
Upper yield strength σ_{uyc}	22.4 ksi	154 MPa
Lower yield strength σ_{tyc}	12 ksi	82.7 MPa
0.02 % yield strength σ_{y2}	15.5 ksi	106.9 MPa
Ramberg–Osgood α	0.038	0.038
Ramberg–Osgood n	7.53	7.53

specimen strain softens and then the material continues to strain while hardening until finally buckling at about 30 ksi (207 MPa) and 40 % engineering strain.

THERMAL AND MECHANICAL REJUVENATION

PEI, similar to other polymers, naturally undergoes a process called physical aging. This process is facilitated by the polymer structure's attempts to attain a state of minimum internal energy. As a result of physical aging, increased force is required in order to promote deformation of the polymer; this process is characterized by an increase in the yield strength and the strain softening regime. Physical aging in polymers has a negative consequence, as it promotes strain softening. During the strain softening regime, polymers exhibit strain localization that cripples the ductility of the material and can cause brittle fracture. To increase the fracture toughness of the material, it is necessary to decrease strain localization and thus decrease the strain softening regime [19,31–34].

Two commonly used processes that work to decrease strain localization in polymers are mechanical and thermal rejuvenation. Mechanical rejuvenation refers to the deformation of the polymer well beyond its yield strength, which lowers the yield strength of the material. Thermal rejuvenation refers to the process of heating a polymer above the glass transition temperature and then quenching the material, causing the polymer chains to return to a high energy state. Mechanical rejuvenation is the more practical of the two processes, but it sacrifices a percentage of total ductility [33,36]. In this experiment, mechanical rejuvenation was accomplished by pre-deforming Ultem 1000 specimens to 12 % strain, and thermal rejuvenation was achieved by heating rod material to 235°C for 30 min and then quenching the material in water to room temperature.

Mechanical and thermal rejuvenation were performed on ASTM D695 compression samples. The mechanical response of PEI to uniaxial compression post-rejuvenation is shown in **Figs. 7(*a*)** and **7(*b*)**. The mechanical and thermal rejuvenation processes were shown to be nearly identical in lowering the yield stress of the material 20 % from 22 ksi (152 MPa) to roughly 18 ksi (124 MPa), and both processes completely eliminated the strain softening regime and thus hindered strain localization. Thermal rejuvenation should be induced under vacuum to prevent the formation of cavities and dimensional changes within the sample. A decrease in ductility amounting to nearly 4 % was induced by mechanical rejuvenation; however, this effect on the ductility was not evident in the experiments, considering that the

FIG. 7

The mechanical response of Ultem 1000 to uniaxial compression subsequent to (a) thermal rejuvenation and (b) mechanical rejuvenation.

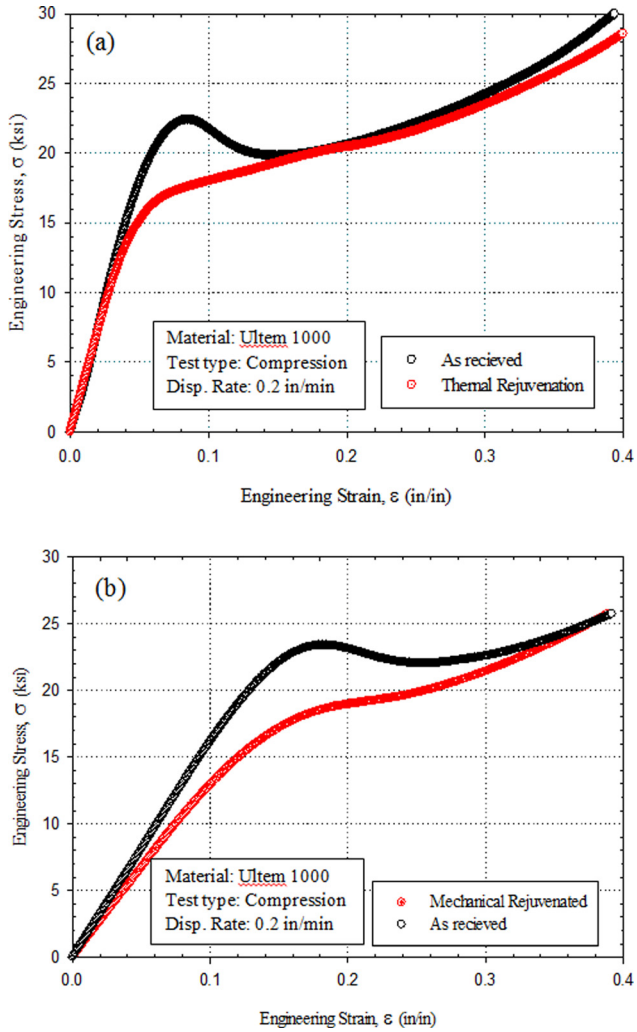

FIG. 8

(a) Standard polyetherimide torsion specimen with dimensions. (b) Testing fixture.

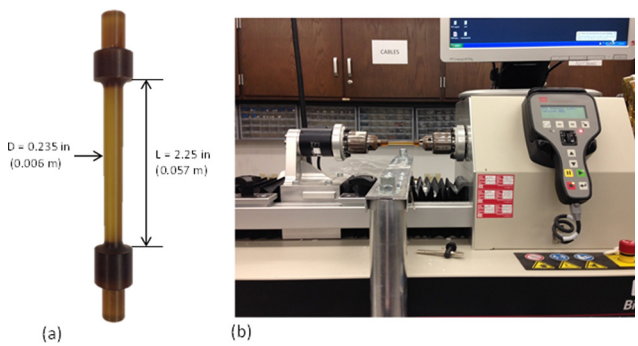

samples buckled before reaching their maximum deformation. Mechanical and thermal rejuvenation were shown to be exceptional methods of reducing the strain softening regime in the response of the material.

Torsion Response

Quasi-static torsion experiments were performed on as-received PEI samples at room temperature. The standard torsion specimen and testing apparatus are illustrated in **Fig. 8**. Samples were machined from rod material to solid cylinders with dimensions corresponding to the specifications of ASTM E143 [37]. The gage length and diameter of the samples measured 2.25 in. (0.057 m) and 0.235 in. (0.006 m), respectively. Experiments were performed on an MTS (Bionix 45 N-m) testing frame at a speed of 5 rpm corresponding to strain rates on the order of 10^{-2}/s.

TEST RESULTS

Similar to the quasi-static deformation of as-received PEI, the material initially responded to shear stress linearly. The elastic response of as-received PEI to torsion loading is presented in **Table 5**, and illustrated in **Fig. 9**. The shear modulus G is the slope of the linear regime and was measured as 174.4 ksi (1.2 GPa). It is expressed as

$$G = \frac{E}{2(1+\nu)} \tag{1}$$

Equation 1 compares the shear and Young's modulus. Poisson's ratio ν was found to be 0.362. The linear regime ceases at the PL, occurring at just over 1 % engineering strain. The response following the linear elastic regime was shown to be nonlinear. At nearly 15 % engineering strain the material exhibited a local maximum in strength; this value was regarded as the yield strength and was measured at 14.0 ksi (96.3 MPa).

Impact Response

The pendulum impact machine first developed by Russel [38] was used with the intention of acquiring the energy absorbed by a sample during deformation. The

TABLE 5

Quasi-static torsion response of Ultem 1000 at room temperature.

Mechanical Properties	Value (English units)	Value (SI units)
Shear modulus G_c	174 ksi	1.20 GPa
Proportional limit PL, %	1.3	1.3
Strain at yield ε_{yt}, %	15.1	15.1
Shear yield strength σ_{sy}	13.96 ksi	96.3 MPa
0.02 % yield strength	6.2 ksi	42.7 MPa
Poisson's ratio ν	0.362	0.362
Ramberg–Osgood α	0.0315	0.0315
Ramberg–Osgood n	4.63	4.63

initial impact machine was later improved and standardized by Charpy [39]. The Charpy impact experiment is now widely used to determine differences in fracture toughness between similar materials. Because of the dynamic loading in the presence of a crack, this experiment has been shown to proficiently predict the occurrence of failure mechanisms as either brittle or ductile in several temperature ranges and loading applications.

To study the mechanisms of failure as a response to high-strain-rate deformation, Charpy impact experiments were performed at room temperature using a universal impact test machine (Instron Model SI-1B) on as-received PEI. Plate material was machined into Type A notched impact samples in accordance with ASTM E23 [40], as shown in **Fig. 10**. The samples had a total length L of 2.165 in. (55 mm), a height H of 0.394 in. (10 mm), a thickness T of 0.394 in. (10 mm), a notch depth D of 0.039 in. (1.0 mm), an angle P of 45°, and a radius of the notch R of 0.001 in. (0.25 mm). To evaluate the properties of PEI, the pendulum of the impact test machine was set at a height C_2 of 1.88 ft (0.573 m), resulting in an impact velocity V_p of 11.0 ft/s (3.35 m/s), corresponding to strain rates on the order of 10^2/s. This height corresponds to the lowest possible starting height of the pendulum.

FIG. 9

(a) The mechanical response of PEI to uniaxial torsion at room temperature. (b) Correlation of the elastic response using the Ramberg–Osgood model.

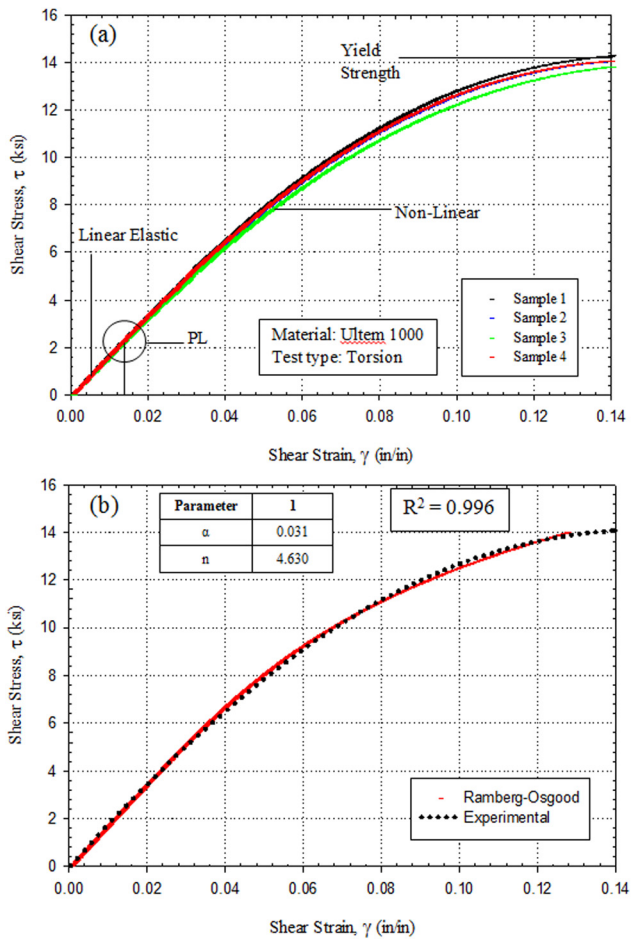

FIG. 10
(a) Type A notched impact sample with dimensions. (b) Charpy impact test machine.

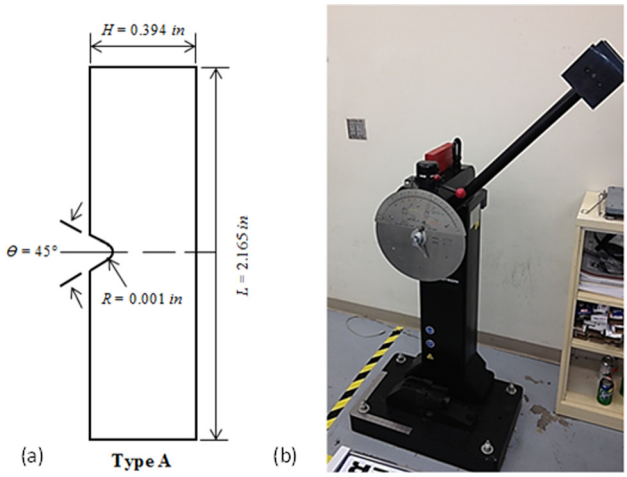

With a pendulum with a mass M_p of 13.3 lb (6.03 kg), the anvil supplied a total impact energy $E_{p'}$ of (25.0 ft-lb) 33.9 J. At this energy, the PEI samples did not absorb any measurable energy. To analyze the failure mechanisms of the samples, we created the macro-scale fracture surface images shown in **Fig. 11**. It can be observed that the samples did not display any lateral expansion, nor did they possess shear lips/area. From the analysis, it can be deduced that in the presence of a notch and at the specified impact energy, PEI will consistently respond to impact with brittle fracture.

High-strain-rate Compression Testing

In order to study the high-strain-rate response of PEI to uniaxial compression at strain rates of 10^2 to 10^5/s, the split Hopkinson pressure bar (SHPB) technique was implemented. Despite the lack of ASTM standards for the use and the design of experiments using the SHPB technique, guidelines and solutions for several design and experimental complications can be found in the *ASM Handbook* [41–43].

BACKGROUND

The SHPB apparatus is implemented as a means of characterizing the dynamic stress-strain behavior of materials. In application, pressures waves transverse a slender bar and impart a dynamic load to an adjacent specimen. Because these devices can generate strain rates on the order of 10^5/s, it is reasonable that conditions similar to explosive detonations or bullet impact can be simulated in a lab-type environment. Although Hopkinson developed the device to study the behavior of waves [44], Davies and Kolsky further developed it in order to attain the constitutive response of a material under high-strain-rate deformation [45,46]. The classic SHPB had three main components: the striker bar, the impact bar, and the transmission bar. The technique has been modified in order to load materials under uniaxial tension, torsion, and bi-axial conditions [47–51].

FIG. 11 (a)–(d) Macro-scale fracture surfaces of Ultem 1000 samples after Charpy impact experimentation. (e) Fracture regions and post-test dimensions of the sample.

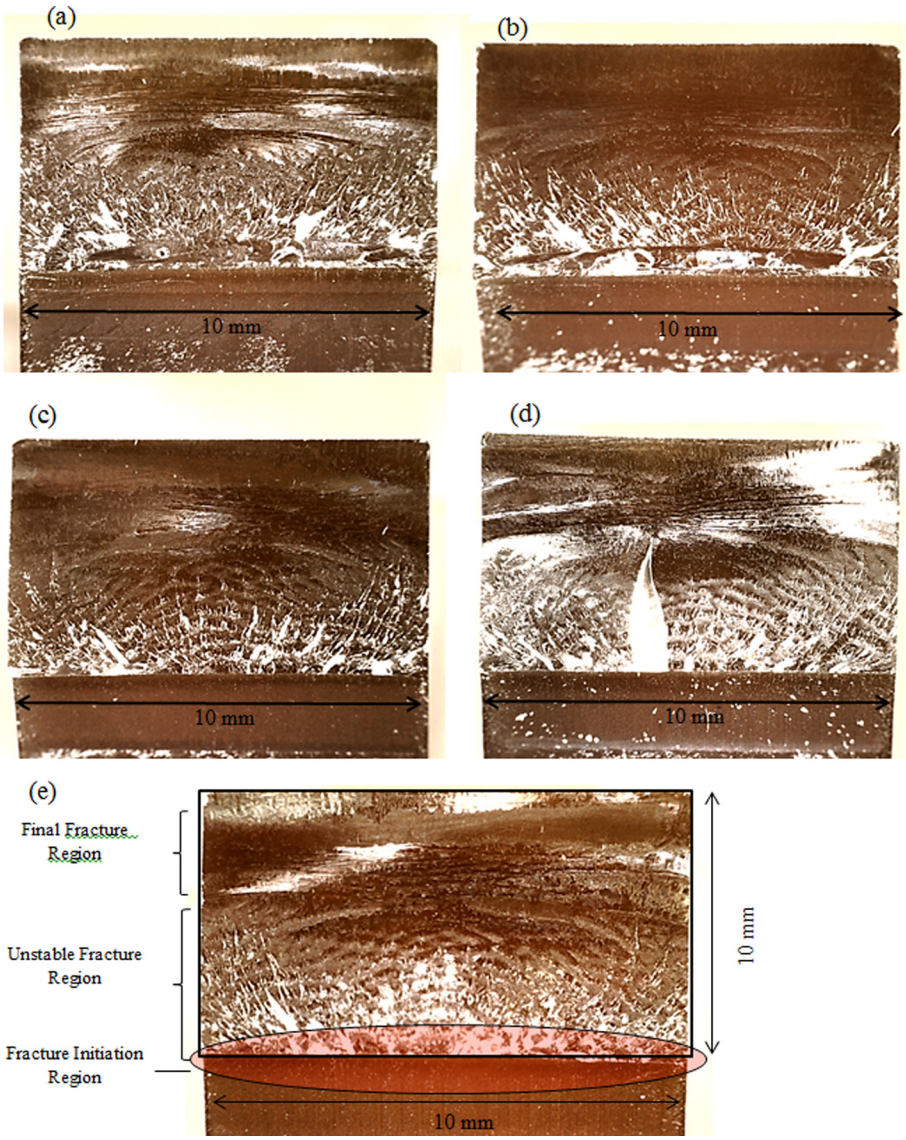

Under compression, a sample located between the incident and transmission bars is compressively loaded by a stress wave generated through the collision of the striker and incident bars. The testing apparatus and specimen are shown in **Figs. 12** and **13**, respectively. Initially, the stress wave, known as the incident pulse ε_I, travels through the incident bar. Once the incident pulse reaches the sample and transmission bar interface, it is partially reflected back through the incident bar, and the remainder travels into the transmission bar. These are referred to as the reflected (ε_r) and transmitted (ε_t) pulses, respectively. The signal acquired from the incident and transmission bars during the experiment is shown in **Fig. 14(*a*)**. The strain rate $\dot{\varepsilon}$ of

FIG. 12
The miniaturized split Hopkinson pressure bar, loaded with polyetherimide samples prior to testing.

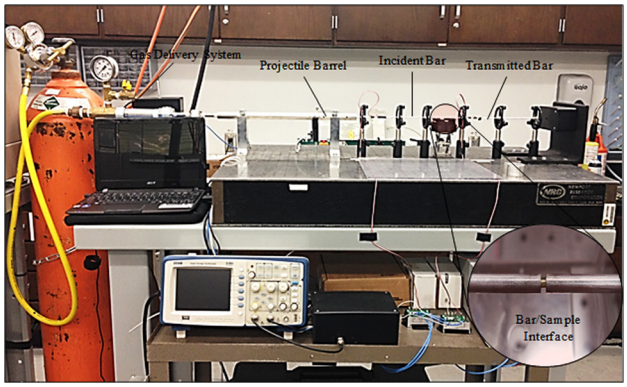

the deforming material can be expressed as a function dependent on the velocity of the bars.

$$\dot{\varepsilon}(t) = \frac{(v_1 - v_2)}{L_{sp}} \tag{2}$$

In Eq 2, v_1 and v_2 are the velocities of the front and back surfaces of the sample, respectively. The velocities of the front and back surfaces of the sample are proportional to the strains generated in the bar and the speed of the propagating wave C_B and are given by

$$V_1 = C_B(\varepsilon_I - \varepsilon_r) \tag{3}$$

$$V_2 = C_B\varepsilon_t \tag{4}$$

FIG. 13 Split Hopkinson pressure bar compression test samples and dimensions.

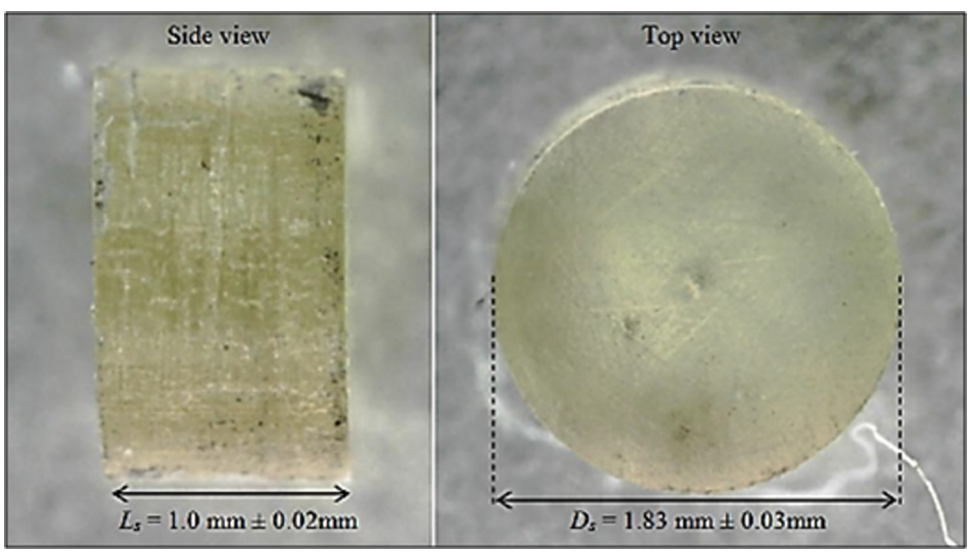

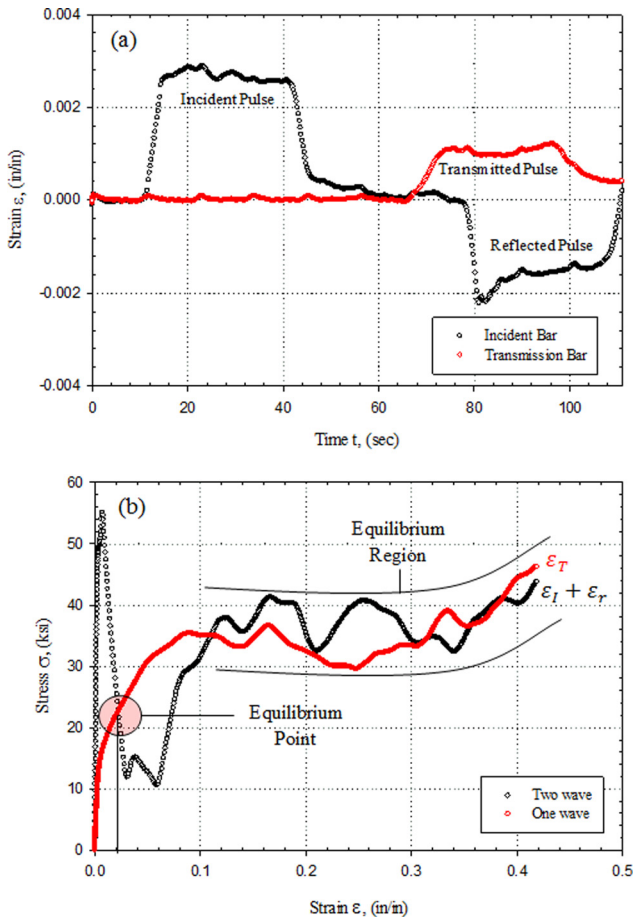

FIG. 14
(a) Acquired signal from the incident and transmitted bars throughout the duration of the miniaturized split Hopkinson pressure bar test. (b) Signals from two-wave and one-wave analysis for dynamic equilibrium check.

When Eqs 3 and 4 are combined into Eq 2, the relationship of the sample deformation speed with the incident, reflected, and transmitted pulses can be expressed as follows:

$$\dot{\varepsilon}(t) = \frac{C_B}{L_{sp}}[\varepsilon_I(t) - \varepsilon_r(t) - \varepsilon_t(t)] \quad (5)$$

When the sample reaches dynamic equilibrium, the strain at the incident bar interface equals that of the transmission bar interface.

$$\varepsilon_I(t) + \varepsilon_r(t) = \varepsilon_t(t) \quad (6)$$

With Eq 6, the equation describing the strain rate of the sample can be simplified to

$$\dot{\varepsilon}(t) = \frac{-2C_B}{L_{sp}}[\varepsilon_r(t)] \quad (7)$$

Finally, using the transmitted strain pulse, the stress on the sample can be described by the following equation:

$$\sigma_s(t) = \frac{EA_b}{A_s}[\varepsilon_t(t)] \quad (8)$$

Under the assumption of dynamic equilibrium, Eqs 7 and 8 can be used to directly acquire the stress and strain rate of the sample as a function of time. The dynamic equilibrium state of the sample can be evaluated by using Eq 8 and replacing $\varepsilon_t(t)$ with $\varepsilon_l(t) + \varepsilon_r(t)$; this evaluation is illustrated in **Fig. 14(*b*)**. Equilibrium was assumed in the region where the summation of the incident and reflected pulses oscillated about the transmitted pulse.

For this experiment, the material was machined to a right circular cylinder using a miniature lathe and then sanded using a custom jig to a diameter D_s of 0.070 in. (1.83 mm) and a length L_{sp} of 0.039 in. (1.00 mm). Specimens with a length-to-diameter ratio of nearly 0.50 were carefully chosen in order to prevent barreling of the samples, radial inertial effects, and interfacial friction between the specimen and bars [46,50,51]. The experiments were conducted using an MSHPB at high strain rates of 10^4/s. The MSHPB is fundamentally identical to the SHPB apart from the reduction in size. A thorough investigation of the MSHPB was conducted by Jia, who elaborated on many of the advantages of the miniaturized setup, such as an increase in the strain-rate limit and a reduction in negative effects of wave dispersion, friction, and inertia [51]. The MSHPB consists of incident and transmitted aluminum 7075-T6 bars, each 10.0 in. (254 mm) in length and 0.125 in. (3.175 mm) in diameter, and a striker bar of the same diameter but 3.00 in. (76.2 mm) in length. Further details about the setup can be found in the thesis by Mutter [52].

RESULTS FROM HIGH-STRAIN-RATE EXPERIMENT

Using the SHPB technique, Ultem 1000 specimens were compressively deformed to nearly 50 % engineering strain at strain rates of roughly 15 000/s. The stress per time response of the sample during impact is shown in **Fig. 15(*a*)**, and the stress-strain curve along with the properties of the curve are presented in **Fig. 15(*b*)** and **Table 6**, respectively. Using Eq 6 in conjunction with Eq 8, the specimens were determined to reach a point of dynamic equilibrium in the range of 2 % to 4 % engineering strain; hence, a linear regression between this point and the point of zero deformation was used to determine a stiffness estimate of the material of 447 ksi (3.08 GPa). This approximation was compared to E of the statically deformed compression samples, and this comparison showed that the elastic response of the sample did not change significantly as a function of strain rate, as shown in **Fig. 15(*c*)**; however, the strength of the material clearly showed strain-rate sensitivity. The material exhibited bilinear behavior in its sensitivity to strain rate and displayed a transition region at around 10^3/s, similar to those of poly(propylene) and poly(vinyl chloride) [4]; this result is illustrated in **Fig. 15(*d*)**. The upper yield strength of the material was averaged at 36.1 ksi (248 MPa), and the lower yield strength of the material at 31.0 ksi (213 MPa). These results are significantly greater than those for the statically deformed samples, averaged at 22.4 ksi (154 MPa) and 12.0 ksi (82.7 MPa).

Considering the bilinear trend of the strength sensitivity of PEI to strain rate, this behavior was correlated using the Ree–Eyring equation. The equation takes the following form:

FIG. 15 Comparison between high-strain-rate and quasi-static responses of polyetherimide to uniaxial compressive loading.

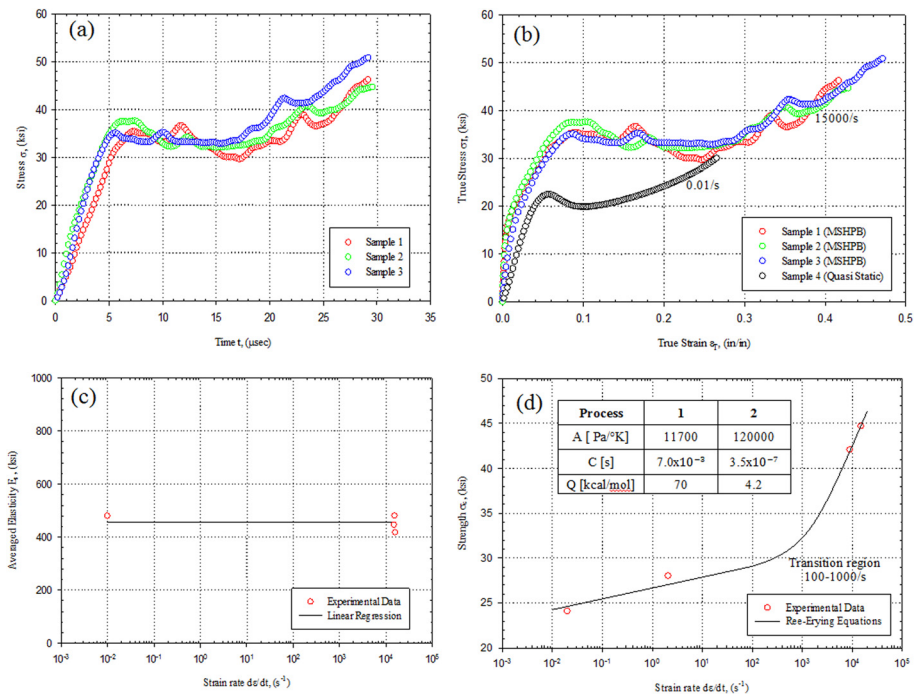

$$\frac{\sigma_y}{\theta} = A_1\left[\ln(2C_1\dot{\varepsilon}) + \frac{Q_1}{R\theta}\right] + A_2\sinh^{-1}\left(C_2\dot{\varepsilon}e^{Q_2/R\theta}\right) \tag{9}$$

where:

A_i = material parameter, Pa/°K,

C_t = material parameter, s,

Q_i = activation energies associated with each process, kcal/mol,

R = universal gas constant, and

θ = absolute temperature of the material [7].

The parameters of the model were determined by fitting experimental data and are shown in **Fig. 15(*d*)**. The results show that the deformation response of this

TABLE 6

Compressive response of Ultem 1000 at 15 000/s strain rate and at room temperature.

Mechanical Properties	Value (English Units)	Value (SI Units)
Average elasticity E_c	480 ksi	3.3 GPa
Strain at yield ε_{yc}, %	8.5	8.5
Upper yield strength σ_{uyc}	36.1 ksi	248 MPa
Lower yield strength σ_{lyc}	31 ksi	213 MPa
Material parameters A_1, A_2	1.70, 1.74 psi/°K	11.7, 12.0 KPa/°K
Activation energy Q_1, Q_2	70.0, 4.20 kcal/mol	70.0, 4.20 kcal/mol
Material parameters C_1, C_2	7.00, 35.0×10^{-7} s	7.00, 35.0×10^{-7} s

material at higher strain rates followed a shape similar to that of the statically deformed specimen, but at an amplified stress. The strength of the material at a strain rate of 15 000/s was shown to be as much as 170 % that of the quasi-static case.

Constitutive Modeling

QUASI-STATIC COMPRESSION OF REJUVENATED MATERIAL

In order to determine the mechanical response of the rejuvenated PEI to quasi-static loading, a model was implemented by using the Ramberg–Osgood strain equation in conjunction with a novel model. The implementation of this model is practical for correlating the behavior of the material, as well as for finding uncertainties within a set of data. The Ramberg–Osgood strain equation was used to model the elastic regime of the material because of the ease of determining the parameters to fit the curve. The equation takes the form

$$\varepsilon = \frac{\sigma}{E} + \alpha\left(\frac{\sigma_o}{E}\right)\left(\frac{\sigma}{\sigma_o}\right)^n \tag{10}$$

where:

σ_o = 0.02 % offset yield stress, and

α and n = parameters that describe the yield point and hardening behavior of the material.

In evaluating the equation at the yield strain ε_o, α is expressed as

$$\alpha = \left(\frac{E\varepsilon_o}{\sigma_o}\right) - 1 \tag{11}$$

The equation can be further evaluated at an arbitrary stress σ_1 and rearranged to solve for the parameter n. The equation is as follows:

$$n = \frac{\ln\left[\frac{E}{\sigma_o\alpha}\left(\varepsilon_1 - \frac{\sigma_1}{E}\right)\right]}{\ln\left(\frac{\sigma_1}{\sigma_o}\right)} \tag{12}$$

Using the parameters α and n (0.053 and 11.92, respectively), the Ramberg–Osgood model was used to fit the elastic regime of the rejuvenated material response to compression, as shown in **Fig. 16(*a*)**. This model was also used to correlate the elastic response of as-received PEI to quasi-static tension, torsion, and compression. The material and hardening constants for these quasi-static cases can be found in Tables **3** through **5**, and the result is illustrated in **Fig. 16(*b*)**. The Ramberg–Osgood model provided an excellent fit for the data and validated the model's ability to capture the elastic response of PEI.

Although the Ramberg–Osgood model correlated well with the material deformation up to 12 % engineering strain, it did not accurately capture the strain hardening response. In order to capture hardening of the material at higher strains, a more sophisticated model was required. Hooke's Law was used to model the initial linear response of the material, and an inverse exponential equation was added in

FIG. 16 (a) The elastic response of rejuvenated PEI fit with the Ramberg–Osgood equation. (b) The elastoplastic response of rejuvenated PEI fit with the inverse exponential equation. (c) The elastoplastic response of rejuvenated PEI correlated with the combined equations. (d) The correlated elastic regime of as-received PEI to quasi-static compression, tension, and torsion fit with the Ramberg–Osgood equation.

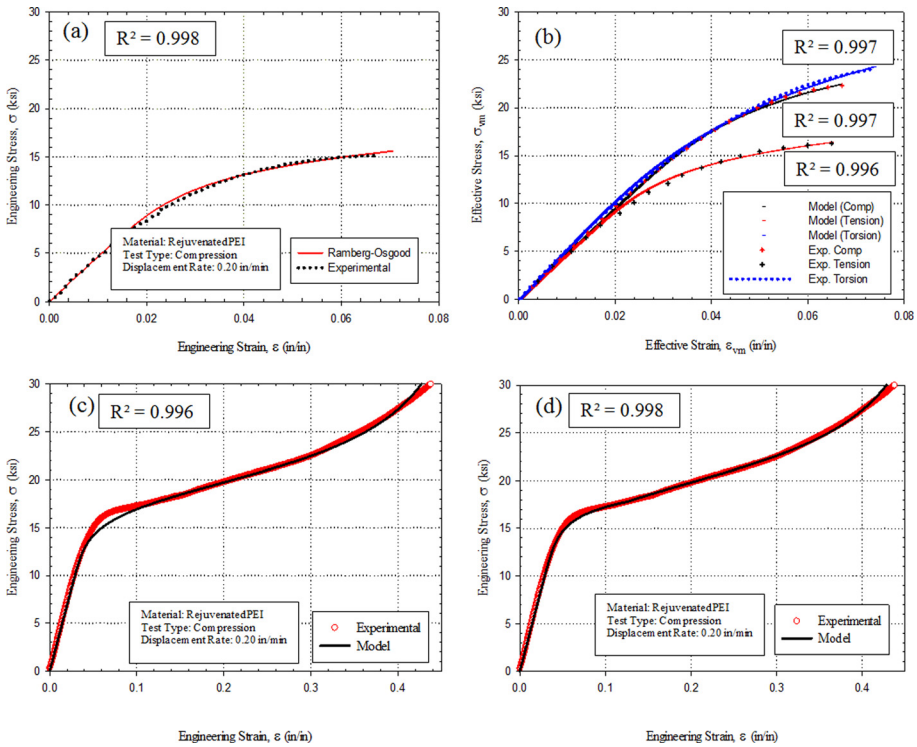

order to model the nonlinear elastic and plastic behavior of the material. The equation becomes

$$\varepsilon = \frac{\sigma}{E} + C_1\left[C_2 + \exp\left(\frac{\sigma_{\text{ref}}}{\sigma}\right)\right]^{-1} \tag{13}$$

where C_1, C_2, and σ_{ref} are model parameters. The model parameters were determined via regression fit. The parameters C_1 and C_2 were found to equal 703 and 1860, respectively, and σ_{ref} was found to be 23.1 ksi (159 MPa), respectively. The result of this model can be seen in **Fig. 16(c)**. Equation 13 correlates well with the elastic and plastic behavior of the material. The maximum error of the model valued at 4.5 % occurred at 0.02 % yield strength.

In order to fully capture the elastic and plastic behavior of the material, a piecewise equation was implemented by combining Eqs 13 and 10. The Ramberg–Osgood equation was used to model the material response until 12 % engineering strain, and an inverse exponential relationship was used to model the material response beyond that point. The piece-wise equation can be expressed as follows:

$$\varepsilon = \begin{cases} \frac{\sigma}{E} + \alpha\left(\frac{\sigma_o}{E}\right)\left(\frac{\sigma}{\sigma_o}\right)^n & 0 \le \varepsilon \le 0.12 \\ \frac{\sigma}{E} + C_1\left[C_2 + \exp\left(\frac{\sigma_{\text{ref}}}{\sigma}\right)\right]^{-1} & 0.12 < \varepsilon \le 0.40 \end{cases} \tag{14}$$

When the Ramberg–Osgood equation and the inverse exponential equation are combined, the elastic and plastic response of PEI in static conditions is accurately captured for deformations at up to 40 % strain. This model bears resemblance to the Voce one-dimensional plastic hardening model, a practical model with three parameters in which plastic strain is inversely related to the stress on the material [53,54]. The elastic response of as-received PEI was correlated solely using the Ramberg–Osgood equation and is provided in **Fig. 16(*d*)**. Future modifications to Eq 14 will be investigated in order to correlate the elastoplastic response of rejuvenated and as-received PEI to multiple rate conditions.

Conclusion

The mechanical response of PEI was evaluated at a range of strain rates and loading conditions. The response of PEI to quasi-static uniaxial tension and compression was found to be consistent with that of other amorphous polymers tested in similar conditions. PEI responds to this loading type by deforming in four distinct mechanical regimes: linear elastic, nonlinear elastic, strain softening, and strain hardening. The as-received PEI material exhibited an upper yield strength characterized by a local maximum in the strength curve; this attribute is a result of physical aging, which promotes strain localization within the material and, as a consequence, leads to strain softening. It was shown that the strain softening regime could be prevented by the induction of either mechanical or thermal rejuvenation. Both processes successfully eliminated the strain softening response of PEI and lowered the yield strength of the material nearly 20 %. The mechanical response of rejuvenated PEI was investigated and correlated using a combination of the Ramberg–Osgood model and an inverse exponential equation. This model accurately predicted the response of PEI for deformations of up to 40 %. The elastic response of PEI to quasi-static torsion was investigated and found to follow a trend similar to that in the tension and compression case. The shear modulus was measured and compared to the Young's modulus in order to evaluate the Poisson's ratio, which was found to be 0.36. The elastic response of PEI was successfully modeled using the Ramberg–Osgood equation. Next, the failure mechanism of PEI was evaluated under dynamic conditions using a Charpy impact test machine, and the material failed predictably and in a brittle manner under the presence of a notch at impact energies of 33.9 J. Finally, the response of PEI to uniaxial compression was evaluated at a strain rate of over 10^4/s using an MSHPB. The stiffness of PEI was found to be independent of strain rate, but the strength of the material was found to be strain-rate sensitive. The strength of PEI increased by 70 % during the high-strain-rate experiments relative to the quasi-static case. The strain-rate sensitivity of PEI was found to be bilinear and was successfully correlated using the Ree–Eyring equation.

ACKNOWLEDGMENTS

Both Bryan Zuanetti and Nathan Mutter are thankful for the support from the University of Central Florida Burnett Honors College in their pursuit of the Honors in the Major undergraduate thesis. Ali P. Gordon is thankful for the collaboration with George Sunny and the Air Force Research Laboratory, Munitions Directorate at Eglin Air Force Base, FL.

References

[1] Chou, S. C., "The Effect of Strain Rate and Heat Developed during Deformation on the Stress-Strain Curve of Plastics," *Exp. Mech.*, Vol 13, No. 10, 1973, pp. 422–432.

[2] Walley, S. M., "A Study of the Rapid Deformation Behaviour of a Range of Polymers," *Philos. Trans. R. Soc. London, Series A: Math. Phys. Sci.*, Vol. 328, No. 1597, 1989, pp. 1–33.

[3] Walley, S. M., "A Comparison of the High Strain Rate Behaviour in Compression of Polymers at 300 K and 100 K," *J. Phys. IV (Colloque)*, Vol. 1, No. 3, 1991, pp. 185–190.

[4] Walley, S. M., "The Rapid Deformation Behaviour of Various Polymers," *J. Phys.*, Vol. 3, No. 12, 1991, pp. 1889–1925.

[5] Eyring, H., "Viscosity, Plasticity and Diffusion as Examples of Absolute Reaction Rates," *J. Chem. Phys.*, Vol. 4, 1936, pp. 283–291.

[6] Bauwens Crowet, C., "Tensile Yield-Stress Behaviour of Glassy Polymers," *J. Polym. Sci. Part A-2, Polym. Phys.*, Vol. 7, No. 4, 1969, pp. 735–742.

[7] Ree, T., "Theory Non-Newtonian Flow Solution System of High Polymers," *J. Appl. Phys.*, Vol. 26, No. 7, 1955, pp. 800–809.

[8] Roetling, J., "Yield Stress Behavior of Poly(ethyl methacrylate) in the Glass Transition Region," *Polymer*, Vol. 6, No. 11, 1965, pp. 615–619.

[9] Beland, S., *High Performance Thermoplastic Resins and Their Composites*, Noyes Data Corporation, Park Ridge, NJ, 1990, pp. 44–45.

[10] Schossig, M., Bierogel, C., and Grellmann, W., "Mechanical Behavior of Glass-fiber Reinforced Thermoplastic Materials Under High Strain Rates," *Polym. Test.*, Vol. 27, No. 7, 2008, pp. 893–900.

[11] Swallowe, G. M., *Mechanical Properties and Testing of Polymers: An A-Z Reference*, Kluwer Academic, London, 1999.

[12] Bijwe, J., "Friction and Wear Studies of Bulk Polyetherimide," *J. Polym. Sci.*, Vol. 25, No. 1, 1990, 2006, pp. 548–556.

[13] Facca, A., "Predicting the Elastic Modulus of Hybrid Fibre Reinforced Thermoplastics," *Polym. Polym. Compos.*, Vol. 14, No. 3, 2006, pp. 239–250.

[14] Smmazcelik, T., Arici, A., and Gunay, V., "Impact-fatigue Behavior of Unidirectional Carbon Fibre Reinforced Polyetherimide (PEI) Composites," *J. Mater. Sci.*, Vol. 41, No. 19, 2006, pp. 6237–6244.

[15] Chen, B., Su, C., Tseng, M., and Tsay, S., "Preparation of Polyetherimide Nanocomposites with Improved Thermal, Mechanical and Dielectric Properties," *Polym. Bull.*, Vol. 57, No. 5, 2006, p. 671.

[16] Bansal, A., Jiang, K., and Schandler, S. L., "Mechanical Properties of Polyetherimide-Alumina Nanocomposites," *SEM Annual Conference and Exposition on Experimental and Applied Mechanics*, Renselear Nanotechnology Center and Department of Material Science and Engineering, Renselear Polytechnic University, 2002.

[17] Zhou, C., Vaccaro, N., Sundarram, S., and Li, W., "Fabrication and Characterization of Polyetherimide Nanofoams Using Supercritical CO2," *J. Cell. Plastics*, Vol. 48, No. 3, 2012, pp. 239–255.

[18] Vina, J., Castrillo, M. A., Arguelles, A., and Vina, I., "A Comparison between the Static and Fatigue Properties of Glass-fiber and Carbon-fiber Reinforced Polyetherimide Composites after Prolonged Aging," *J. Polym. Compos.*, Vol 23, No. 4, 2002, pp. 619–623.

[19] García, M. A., Castrillo, M. A., Arguelles, A., and Vina, J., "Effects of Natural Aging for Eight Years on Static Properties of Glass or Carbon Fibre Reinforced Polyetherimide," *Corros. Eng. Sci. Technol.*, Vol. 42.1, 2007, pp. 61–63.

[20] Ames, N. M. and Anand, L., "A Theory of Amorphous Polymeric Solids Undergoing Large Deformations: Application to Micro-indentation of Poly(methyl methacrylate)," *Int. J. Solids Struct.*, Vol. 40, No. 6, 2003, pp. 1465–1487.

[21] Boyce, M., Socrate, S., and Llana, P., "Constitutive Model for the Finite Deformation Stress–Strain Behavior of Poly(ethyleneterephthalate) above the Glass Transition," *Polymer*, Vol. 41, 2000, pp. 2183–2201.

[22] Mulliken, A. D., 2006, "Mechanics of Amorphous Polymers and Polymer Nanocomposites During High Rate Deformation," Ph.D. thesis, Massachusetts Institute of Technology, Cambridge, MA.

[23] Pecht, M., "Characterization of Polyimides Used in Ge High Density Interconnects," *7th International SAMPE Electronics Conference*, University of Maryland, College Park, MD, June 20–23, 1994, pp. 432–445.

[24] Siviour, C. R., "The High Strain Rate Compressive Behaviour of Polycarbonate and Polyvinylidene Difluoride," *Polymer*, Vol. 46, No. 26, 2005, pp. 12546–12555.

[25] Chou, S. C., "The Effect of Strain Rate and Heat Developed during Deformation on the Stress-Strain Curve of Plastics," *Exp. Mech.*, Vol. 13, No. 10, 1973, pp. 422–432.

[26] ASTM D638: Standard Test Method for Tensile Properties of Plastics, *Annual Book of ASTM Standards*, ASTM International, West Conshohocken, PA, 2010.

[27] ASTM E83-10a: Standard Practice for Verification and Classification of Extensometer Systems, *Annual Book of ASTM Standards*, ASTM International, West Conshohocken, PA, 2010.

[28] Brown, N. and Ward, I. M., "Load Drop at Upper Yield Point of Polymer," *J. Polym. Sci.*, Vol. 6, No. 5, 1968, pp. 607–620.

[29] Jordan, J. L., Foley, J. R., and Siviour, C. R., "Mechanical Properties of Epon 826/DEA Epoxy," *Mech. Time Depend. Mater.*, Vol 12, No. 3, 2008, pp. 249–272.

[30] Prakash, V. and Mehta, N., "Uniaxial Compression and Combined Compression-and-shear Response of Amorphous Polycarbonate at High Loading Rates," *Polym. Eng. Sci.*, Vol. 52, No. 6, 2012, pp. 1217–1231.

[31] Struik, L. C. E., *Physical Aging in Amorphous Polymers and Other Materials*, Elsevier, New York, 1978.

[32] Simon, S., Plazek, D., Sobieski, J., and McGregor, E., "Physical Aging of a Polyetherimide: Volume Recovery and Its Comparison to Creep and Enthalpy Measurements," *J. Polym. Sci. Part B Polym. Phys.*, Vol. 35, No. 6, 1996, pp. 929–936.

[33] Mahajan, D., Estevez, R., and Basu, S., "Ageing and Rejuvenation in Glassy Amorphous Polymers," *J. Mech. Phys. Solids*, Vol. 58, No. 10, 2010, pp. 1474–1488.

[34] Marano, C. and Rink, M., "Viscoelasticity and Shear Yielding Onset in Amorphous Glassy Polymers," *Mech. Time Depend. Mater.*, Vol. 10.3, 2013, pp. 173–184.

[35] ASTM D695: Standard Test Method for Compressive Properties of Rigid Plastics, *Annual Book of ASTM Standards*, ASTM International, West Conshohocken, PA, 2010.

[36] Kierkels, J. T. A., *Tailoring the Mechanical Properties of Amorphous Polymers*, Technische University of Eindhoven, Eindhoven, Netherlands, 2006.

[37] ASTM E143, "Standard Test Method For Shear Modulus at Room Temperature," *Annual Book of ASTM Standards*, ASTM International, West Conshohocken, PA, 2008.

[38] Russell, S. B., "Experiments with a New Machine for Testing Materials by Impact," *Trans. ASCE*, Vol. 39, 1898, pp. 237–250.

[39] Charpy, M. G., "Note sur l'Essai des Metaux a la Flexion par Choc de Barreau Entailles [Note on Testing Metals to Impact Bending of Notch]," *Societe de Ingenieurs Francais*, Vol. 1, p. 848, 1901 (in French).

[40] ASTM E23: Standard Test Methods for Notched Bar Impact Testing of Metallic Materials, *Annual Book of ASTM Standards*, ASTM International, West Conshohocken, PA, 2012.

[41] Chen, W. W. and Song, B., *Split Hopkinson (Kolsky) Bar: Design, Testing and Applications*, Mechanical Engineering Series, Springer, New York, 2011.

[42] Gray, G. T., III, "Classic Split-Hopkinson Pressure Bar Testing," *ASM Handbook, Volume 8: Mechanical Testing and Evaluation*, ASM International, Materials Park, OH, 2000, pp. 463–476.

[43] Gray, G. T., III and Blumenthal, W. R., "Split-Hopkinson Pressure Bar Testing of Soft Materials," *ASM Handbook, Volume 8: Mechanical Testing and Evaluation*, ASM International, Materials Park, OH, 2000, pp. 488–496.

[44] Hopkinson, B., "A Method of Measuring the Pressure Produced in the Detonation of High Explosives or by the Impact of Bullets," *Philos. Trans. R. Soc. London*, Vol. 213, No. 497–508, 1914, p. 19.

[45] Kolsky, H., "An Investigation of the Mechanical Properties of Materials at Very High Rates of Loading," *Proc. Phys. Soc.*, Vol. 62, No. 11, 1949, pp. 676–700.

[46] Davies, R. M., "Critical Study of Hopkinson Pressure Bar," *R. Soc. London Philos. Trans. Series*, Vol. 240, 1948, pp. 376–457.

[47] Harding, J., "Tensile Testing of Materials at Impact Rates of Strain," *Proc. Inst. Mech. Eng. Part C: J. Mech. Eng. Sci.*, Vol. 2, 1960, pp. 88–96.

[48] Gilat, A., "Torsional Split Hopkinson Bar Tests at Strain Rates Above 10^4," *Exp. Mech.*, Vol. 40, No. 1, 2000, pp. 54–59.

[49] Nemat-Nasser, S., Isaacs, J., and Rome, J., "Triaxial Hopkinson Techniques," *ASM Handbook of Mechanical Testing and Evaluation*, Vol. 8, ASM International, Materials Park, OH, 2000, pp. 516–518.

[50] Gray, G. T., Blumenthal, W. R., Trujillo, C. P., and Carpenter, R. W., "Influence of Temperature and Strain Rate on the Mechanical Behavior of Adiprene L-100," *J. Physique*, Vol. 7, 1977, pp. 523–528.

[51] Jia, D., "A Rigorous Assessment of the Benefits of Miniaturization in the Kolsky Bar System," *Exp. Mech.*, Vol. 44, No. 5, 2004, pp. 445–454.

[52] Mutter, N., 2010, "Characterization of Dynamic and Static Behavior of Polyetherimide," M.S. thesis, University of Central Florida, Orlando, FL.

[53] Voce, E., "The Relationship Between Stress and Strain for Homogenous Deformation," *J. Inst. Metallurg.*, Vol. 74, 1948, pp. 537–562.

[54] Voce, E., "A Practical Strain Hardening Function," *J. Inst. Metallurg.*, Vol. 51, 1955, pp. 219–226.